



The Effect of highly dispersed oxidized multi-walled carbon nanotubes on the performance of PVDF/PVC ultrafiltration membrane

Masoumeh Norouzi^a, Majid Pakizeh^{a,*}, Mahdieh Namvar-Mahboub^b

^aFaculty of Engineering, Department of Chemical Engineering, Ferdowsi University of Mashhad, P.O. Box 9177948974, Mashhad, Iran, Tel. +98 51 38816840; email: masume_noroozi@yahoo.com (M. Norouzi), Tel./Fax: +98 51 38816840; email: Pakizeh@um.ac.ir (M. Pakizeh)

^bDepartment of Chemical Engineering, University of Gonabad, Gonabad, Iran, Tel./Fax: +98 51 38816840; email: namvarmahboob@yahoo.com

Received 15 September 2015; Accepted 26 January 2016

ABSTRACT

In this study, functionalized multi-walled carbon nanotubes (F-MWCNTs) were used to modify the polyvinylidene fluoride (PVDF)/polyvinyl chloride (PVC) blend UF membrane via solution blending method. The effect of F-MWCNTs dosage (0–1%) on the properties and performance of PVDF/PVC/F-MWCNTs membranes was investigated. The prepared blend membranes were characterized by Fourier Transform Infrared spectroscopy (FT-IR), Scanning Electron Microscopy (SEM), Field Emission Scanning Electron Microscopy (FESEM), contact angle, and tensile strength techniques. Results showed that hydrophilicity of membranes was enhanced with increase of F-MWCNTs content. The performance of the membranes was evaluated in terms of pure water flux (PWF) and dextran filtration. The results showed that presence of F-MWCNTs in polymer matrix improved performance and antifouling properties of PVDF/PVC blend membrane. Accordingly, incorporation of 0.3–0.5 wt.% of F-MWCNTs represented maximum dextran rejection and permeate flux, respectively.

Keywords: Functionalized multi-wall carbon nanotube; Ultrafiltration; Hydrophilicity; Antifouling

1. Introduction

On account of its good chemical resistance, mechanical properties and thermal stability of polyvinylidene fluoride (PVDF) has received much attention as a membrane material. The use of pure PVDF membrane for ultrafiltration (UF) of aqueous solutions has been limited due to its hydrophobic nature, which causes membrane fouling. Many studies have been carried out to enhance the hydrophilicity

and performance of PVDF membrane. Regularly, surface modification or blending modification methods are used to improve antifouling properties of UF membranes [1]. In the case of blending modification technique, polymer is blended with the modifying agent to attain the desired functional properties in the membrane structure. Therefore, the preparation and modification processes can be accomplished in a single step. This feature introduces solution blending as a convenient membrane modification method. Up to now, polymers [2–6], amphiphilic copolymers [7,8],

*Corresponding author.

and inorganic particles [9–12] are applied to modify the pure PVDF membrane.

Among the polymers which can be used as modifier, PVC has gained attention due to its outstanding properties including: robust mechanical strength, low cost, high resistance to acids, bases, solvents, and chlorine [13,14]. Although both PVC and PVDF membranes have excellent UF separation performance, PVC has economical superiority when compared with PVDF. Thus, it can be good candidate to improve properties of PVDF membrane for UF process. Accordingly, Zhang et al. [15] studied the effect of PVC/PVDF ratio (0–1) on performance of PVDF/PVC blend membrane. They found that 50% of PVC enhanced water flux of prepared membrane up to 19 times when compared with that one of pure PVDF membrane. However, PVDF/PVC blend membrane showed lower mechanical stability because of their more porous structure than pure PVDF membrane.

It has also been proven that dispersion of inorganic nanoparticles in the polymer matrix is also useful in the improvement of blend membrane performance [16]. Thanks to their exclusive natural properties, carbon nanotubes (CNTs) are one of the inorganic materials which can be used to prepare new generation of composite membranes [17–19]. The CNTs represent extremely high mechanical strength, high thermal and electrical conductivity, low density and especially high specific area [20,21]. Anyhow, uniform dispersion of CNTs and their appropriate adhesion to polymer chains can be achieved subsequent to functionalization by chemical agents [22–24]. There are some literatures which have been carried out in the field of membrane preparation by introducing F-MWCNTs to PVDF matrix [25,26]. Zhao et al. [25] functionalized MWCNTs using grafted hyperbranched poly (amine–ester). They incorporated different amount of prepared F-MWCNTs (0–2%) into PVDF matrix to improve performance of PVDF membrane. Their results indicated that at 1.5% of F-MWCNTs, permeate flux increased from about $1 \text{ L m}^{-2} \text{ h}^{-1}$ for pure PVDF to $5 \text{ L m}^{-2} \text{ h}^{-1}$ for PVDF/F-MWCNTs membrane, while BSA rejection shift down 5%. In addition, according to the Flux recovery (FR) values, one can conclude that the presence of F-MWCNTs improved antifouling properties of PVDF membrane. Zhang et al. [26] investigated the effect of oxidized-multi-walled carbon nanotubes (O-MWNTs) on the performance of PVDF/perfluorosulfonic acid (PFSA) hollow fiber membrane. They showed that surface hydrophilicity, porosity, and permeation flux of resultant mixed matrix membranes were evidently improved by the addition of O-MWNTs. These findings reveal that utilizing F-MWCNTs as an additive

into PVDF matrix can improve the hydrophilicity, water permeability, and the antifouling ability of membrane. To our best knowledge, there is no information on the effect of combination of both PVC and F-MWCNTs on the performance of PVDF UF membrane.

Based on the above-mentioned considerations, this work is devoted to study properties and performance of PVDF/PVC/F-MWCNTs blend membranes. To do this, raw MWCNTs were acidified to prepare F-MWCNTs and then characterized by Fourier Transform Infrared Spectroscopy (FTIR) analysis. The PVDF/PVC/F-MWCNTs membranes were fabricated via phase inversion method. The prepared mixed matrix membranes were characterized by applying FTIR, Scanning Electron Microscopy (SEM), tensile strength, porosity, and contact angle tests. In addition, the effects of F-MWCNTs on the separation performance of PVDF/PVC membrane were studied via dextran removal process.

2. Experimental

2.1. Materials

PVDF ($M_w = 534,000 \text{ g/mol}$) and dextran ($M_r = 450,000\text{--}650,000$) were purchased from Sigma-Aldrich (Germany). PVC powder was obtained from Vinytai Co. (Thailand). MWNTs (purity 95%) with an average length of $30 \mu\text{m}$ and a diameter of $10\text{--}20 \text{ nm}$ were provided by Shenzhen Nano-Tech Port Co. DMF and HNO_3 (67%) employed as solvent was purchased from Merck. Distilled water was used as nonsolvent for the casting solution. H_2SO_4 (95–98%) was supplied from Arman Sina (Iran). PTFE filtration membranes (pore size of $0.2 \mu\text{m}$) were acquired from Whatman Company.

2.2. Functionalization of MWCNTs

Acidification process was conducted to introduce hydrophilic functional groups onto the surface of MWCNTs. According to the functionalization procedure, 2 g of raw MWCNTs were soaked in 160 mL solution of $\text{H}_2\text{SO}_4/\text{HNO}_3$ (3/1 in vol.%) and then were heated to 70°C for 8 h without stirring [27]. The as-prepared solution was diluted with 2 L deionized water and filtered through a PTFE membrane. The resultant F-MWCNTs were washed with deionized water and dried at 60°C in an oven for 6 h. It should be notified that this procedure assists removal of the existed metallic catalyst particles and amorphous carbon as the impurities of raw MWCNTs.

2.3. Membrane preparation

The PVDF/PVC/F-MWCNTs membranes were prepared by solution blending and immersion precipitation techniques. Different amounts of F-MWCNTs (0–1% weight/weight of polymers) were added into a certain amount of DMF (81 wt.%) and then sonicated for 30 min to ensure well dispersion. Afterward, PVDF and PVC (1:1 in wt.%) were dissolved in the dispersed solutions by magnetic stirrer at 80°C for 24 h and then were kept for the removal of bubbles. The homogeneous solutions were cast on a glass plate using casting bar (Neurtek2281205) with adjusted thickness of 250 μm . The resultant films were allowed being in atmosphere for 30 s for solvent evaporation. Then, they were immersed into a water coagulation bath for 1 d to ensure an adequate solvent–nonsolvent exchange. The as-prepared mixed matrix membranes were nominated according to the composition of casting solution as shown in Table 1.

2.4. Characterization

2.4.1. FT-IR analysis

FTIR spectrometer (Thermo Nicolet Avatar 370) was applied to evaluate successful functionalization of raw MWCNTs. Additionally, the effect of F-MWCNTs on the chemical structure of PVDF/PVC/F-MWCNTs membranes was investigated. For all samples, FTIR spectra were collected over wavenumber range of 500–4,000 cm^{-1} with a spectral resolution of 1 cm^{-1} .

2.4.2. Morphological studies

In order to inspect cross-sectional morphology of the mixed matrix membranes, SEM (LEO1450VP, Zeiss, Germany) was employed. The membranes were cut into pieces of small sizes and then were immersed in liquid nitrogen. Frozen bits of the membranes were properly broken. Finally, samples with clean cut edges

were gold sputtered for producing electric conductivity. In order to observe MWCNTs on the surface of membranes, Field Emission Scanning Electron Microscopy (FESEM, ZIGMA/VP, Zeiss, Germany) was used.

2.4.3. Contact angle measurement

The surface contact angle of PVDF/PVC/F-MWCNTs membranes was measured using OCA15 Plus analyzer (Germany). To minimize the experimental error, the average contact angle at four random sites of each sample was reported. The obtained contact angle values demonstrate change of hydrophilicity of as-prepared membrane.

2.4.4. Mechanical properties

Universal testing machine (ZWICK-Z250, Germany) was employed to study mechanical stability of the as-prepared membranes through measurement of the tensile strength. All samples were deformed with the speed of 5 mm min^{-1} at room temperature.

2.4.5. Filtration performance

A self-made cross flow filtration cell with effective area of $9.62 \times 10^{-4} \text{ m}^2$ was used to evaluate membrane performance and antifouling properties during separation of dextran. The flux and rejection of all membranes were determined under operating pressure of 3 bar. Dextran solution with concentration of 0.5 g L^{-1} was used as feed.

The permeate flux, J ($\text{L m}^{-2} \text{ h}^{-1}$), was calculated by the following equation (Eq. (1)):

$$J = \frac{V}{A \cdot t} \quad (1)$$

Table 1
Composition of casting solution for PVDF/PVC/F-MWCNTs membranes

Membrane code	PVDF + PVC ^a (wt.%)	$W_{\text{F-MWCNTs}}^{\text{b}}$ (wt.%)
PVDF50	19	0
PVDF50–0.3	19	0.3
PVDF50–0.5	19	0.5
PVDF50–0.7	19	0.7
PVDF50–1	19	1

^a50% PVDF + 50% PVC.

^bMass ratio of F-MWCNTs to PVDF + PVC.

where V (L) is the volume of permeated water, A (m^2) is the effective membrane surface area and t (h) is the permeate collection time.

After steady-state flux was achieved, the chemical oxygen demand (COD) of permeate and feed were measured using the PC checkit COD equipment (Lovibond Co.). In COD measurement method, each sample was exposed to the oxidizing solution, cooled, and then analyzed. To determine dextran rejection during UF process the following equation (Eq. (2)) was applied [28].

$$R = 1 - \frac{COD_{\text{permeate}}}{COD_{\text{feed}}} \quad (2)$$

2.4.6. Analysis of membrane fouling

The FR was used to quantify fouling amount of as-prepared membranes. The method is based on the difference between pure water flux (PWF) before and after separation process. In this case, after filtration of dextran solution, the membranes were washed with distilled water for 20 min. This was followed by estimation of water flux of cleaned membranes J_{w2} ($L m^{-2} h^{-1}$). The FR was calculated as follow:

$$FR(\%) = \left(\frac{J_{w2}}{J_{w1}} \right) \times 100 \quad (3)$$

where J_{w1} is PWF of prepared membranes before separation process. Reversible fouling ratio (R_r) and irreversible fouling ratio (R_{ir}) were also defined and calculated by following equations, respectively.

$$R_r(\%) = \left(\frac{J_{w2} - J_p}{J_{w1}} \right) \times 100 \quad (4)$$

$$R_{ir}(\%) = \left(\frac{J_{w1} - J_{w2}}{J_{w1}} \right) \times 100 \quad (5)$$

where J_{w1} and J_p are PWF and permeate flux of PVDF/PVC/F-MWCNTs membrane, respectively.

3. Results and discussions

3.1. Characterization of F-MWCNTs

The FTIR spectra of raw MWCNTs and F-MWCNTs are presented in Fig. 1. The appearance of band at $1,515 \text{ cm}^{-1}$ is attributed to C=C bond of carbon structure of CNTs. However, for F-MWCNTs, the above-mentioned band is observed at wavenumber of $1,567 \text{ cm}^{-1}$ with strong intensity because of overlapped vibrations of double bonds C=C and carbonyl groups C=O [29]. Besides, new bands are observed at $3,509$,

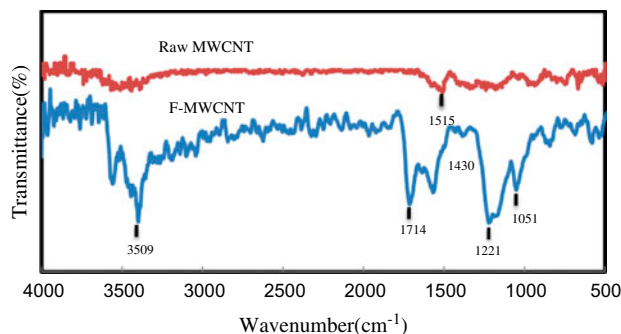


Fig. 1. The FTIR spectra of raw MWNTs and F-MWNTs.

$1,714$, $1,430$, and $1,221 \text{ cm}^{-1}$ which are corresponded to OH, C=O, OH bending vibration of COOH bonds and sulfate groups (OSO_3H), respectively. The band at about $1,051 \text{ cm}^{-1}$ is assigned to the C–O stretching vibration. The increased intensity of the OH band and the appearance of new bands suggest that oxidation procedure of the MWCNTs successfully introduced COOH, OH, CO, and OSO_3H groups onto the walls of the nanotubes [29,30].

Fig. 2 depicts MWNTs/DMF and F-MWCNTs/DMF solutions to compare dispersion quality of MWCNTs before and after modification. As can be seen, F-MWCNTs/DMF solution remained stable for several days after sonication but raw MWNTs precipitated. In fact, the groups on F-MWCNTs surfaces are the main driving force for the uniform dispersion of nanotubes in solvent.

3.2. Characterization of mixed matrix membranes

3.2.1. FTIR analysis

Fig. 3 exhibits the FTIR spectra of the PVDF/PVC membrane and PVDF/PVC/F-MWCNTs membrane with 0.5 wt.% of F-MWCNTs. For PVDF/PVC blend membrane, bands at $1,675$, $1,404$, and $1,235 \text{ cm}^{-1}$ are attributed to $-C=CF_2-$ vibrations of vinylidene group, C–F stretching and very strong mode of $-CF_2-$ ring breathing vibrational modes of PVDF, respectively. The absorption band appearing at 874 cm^{-1} may be assigned to the characteristic frequency of vinylidene compounds. C–Cl stretching frequencies of PVC are found at 641 and 612 cm^{-1} , respectively [31,32]. In the case of PVDF/PVC/F-MWCNTs membrane, a new band is also depicted at $1,740 \text{ cm}^{-1}$, which is not present in the spectrum for the PVDF/PVC membrane. This band is due to the presence of C=O bond stretching in carboxylic acid groups, indicating successful F-MWCNTs immobilization within the functionalized membrane [33].

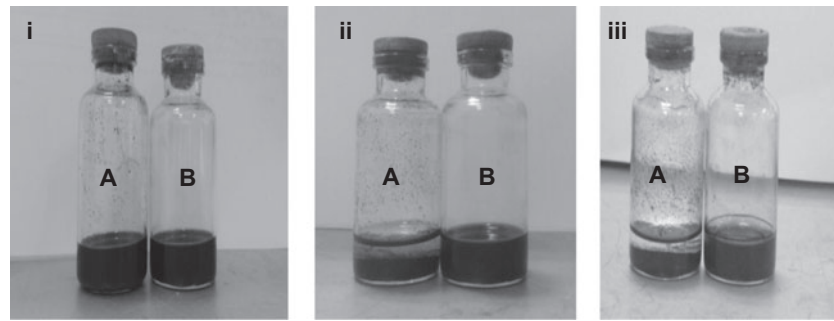


Fig. 2. The dispersion of raw (A) and functionalized (B) MWCNTs in DMF during (i) 30 min, (ii) 7 d, and (iii) 2 month after sonication.

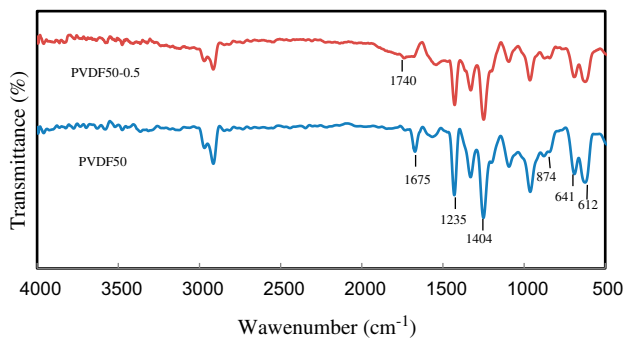


Fig. 3. The FTIR spectra of the PVDF50 and PVDF50–0.5 membranes.

3.2.2. SEM and FESEM analysis

The cross-sectional view of as-prepared membranes was observed by SEM to investigate impact of F-MWCNTs on the structure of PVDF/PVC membrane. As shown in Fig. 4, all membranes display a typical asymmetric membrane structure with a selective top layer and a porous sub-layer. It is found from Fig. 4 that incorporation of F-MWCNTs into blend polymer matrix changes the structure of the PVDF/PVC membrane. As can be seen, for PVDF/PVC membrane, sub-layer includes spherical and finger-like pores (Fig. 4(a)). With increment of the F-MWCNTs dosage from 0 to 0.5 wt.%, size and number of pores increases and sponge-like region of membrane structure decreases. These observed results can be related to the fast exchange of solvent and nonsolvent in the phase inversion process due to the presence of hydrophilic F-MWCNTs in membrane structure [34]. Further increase of F-MWCNTs dosage to 0.7 wt.% leads to formation of less porous sub-layer. Indeed, by increasing F-MWCNTs dosage, viscosity of casting solution increases, which lead to the delayed demixing.

Conversely, solvent–nonsolvent exchange rate increases which causes instantaneous demixing. At high dosages of inorganic filler, the effect of viscosity prevails over hydrophilic nature of F-MWCNTs. Thus, delayed demixing becomes the dominant mechanism of membrane formation and as a result denser structure is observed [35]. Vatanpour et al. [36] observed the same behavior for PES/amine-functionalized MWCNTs nanocomposite membrane. Their results indicated that membranes containing 0.015, 0.03, and 0.045 wt.% of F-MWCNTs had more porous structure, while increasing filler dosage to 0.6 wt.% led to the formation of a thicker top layer.

Fig. 5 presents the surface FESEM images of PVDF50 and PVDF50–0.5 membranes. It is evident from Fig. 5 that F-MWCNTs are dispersed on the surface of the PVDF50–0.5 membrane. Additionally, there is no defect between polymer matrix and F-MWCNTs due to their proper interaction.

3.2.3. Contact angle measurements

The surface hydrophilicity obtained by the contact angle measurement plays a significant role on the flux and antifouling performance of membranes. Generally, the smaller contact angle, the greater is the hydrophilicity [37]. Table 2 shows the contact angle values for PVDF/PVC and PVDF/PVC/F-MWCNTs membranes. As shown in Table 2, the contact angle decreases from 61.20 to 50.26°, while the F-MWCNTs increase from 0 to 1%. This result indicates that the surface hydrophilicity of membranes is improved with the increase of F-MWCNTs content in membrane structure. As mentioned by FESEM images, F-MWCNTs are adequately dispersed on the surface of mixed matrix membranes. In fact, during the immersion precipitation process, hydrophilic

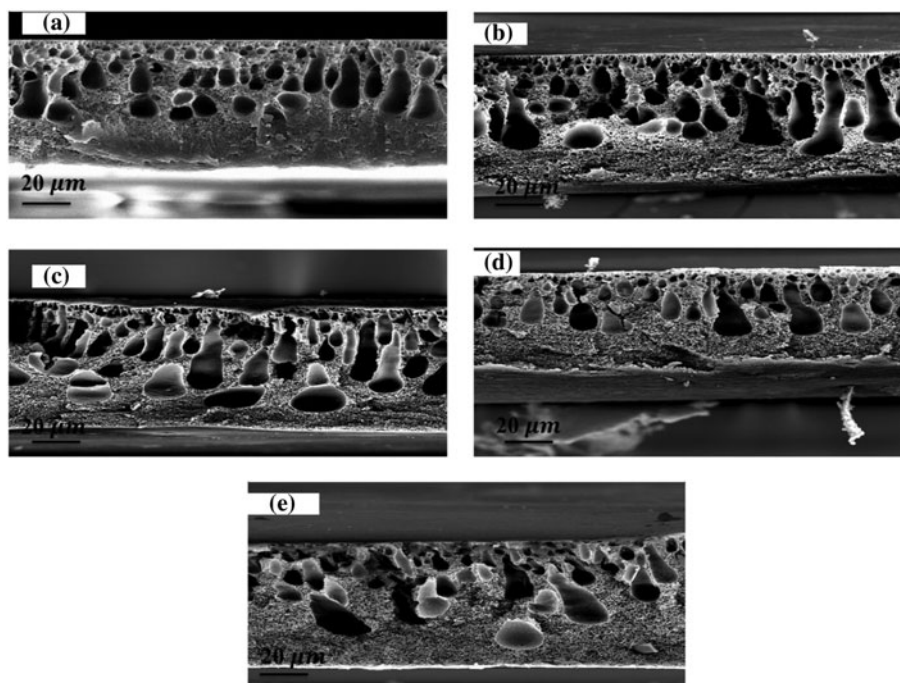


Fig. 4. Effect of F-MWCNTs on cross-sectional SEM images of PVDF/PVC/F-MWCNTs membranes: (a) 0 wt.% F-MWCNTs, (b) 0.3 wt.% F-MWCNTs, (c) 0.5 wt.% F-MWCNTs, (d) 0.7 wt.% F-MWCNTs, and (e) 1 wt.% F-MWCNTs.

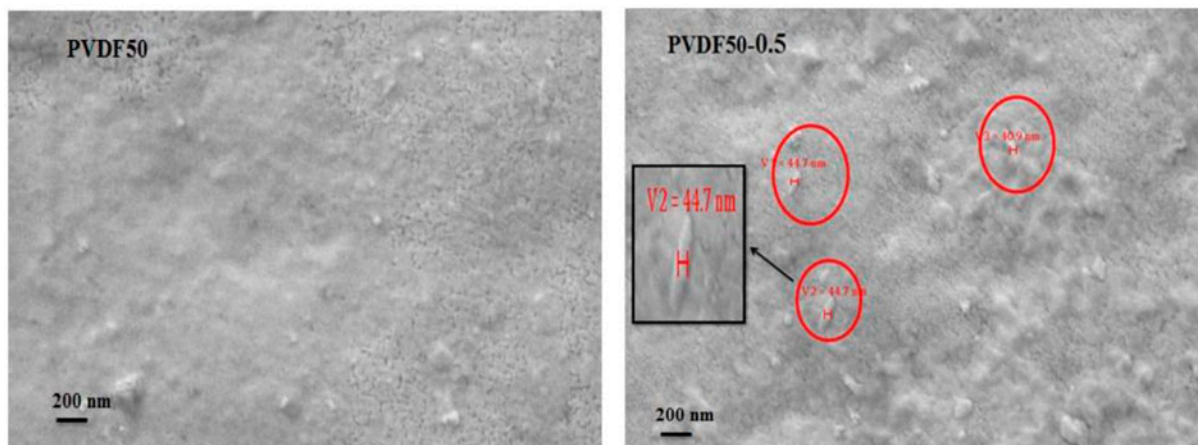


Fig. 5. Surface FESEM images of membranes prepared: (a) PVDF50 and (b) PVDF50–0.5.

MWCNTs migrate upward to reduce the free energy at interface of water and membrane [38]. Thus, the observed trend of contact angle is owed to the presence of the hydrophilic groups of F-MWCNTs on surface of as-prepared membranes.

The presence of F-MWCNTs on membrane surface is also visible in the top and the bottom surface photographs of as-prepared membranes (Fig. 6). Color of bottom surface of membrane is slightly lighter than

that of top surface, signifying the tendency of functionalized MWCNTs to migrate upward.

3.2.4. Tensile strength results

The tensile strength of PVDF/PVC/F-MWCNTs blend membranes as a function of MWCNTs content is shown in Fig. 7. As can be observed, by the addition of F-MWCNTs into PVDF/PVC matrix,

Table 2
Contact angle of prepared membranes

Membrane code	Contact angle (°)
PVDF50	61.20 ± 0.5
PVDF50-0.3	56.44 ± 0.63
PVDF50-0.5	55.00 ± 0.66
PVDF50-0.7	53.11 ± 0.74
PVDF50-1	50.26 ± 0.83

tensile strength reduces. This finding is related to the change of membrane morphology. As stated before, PVDF/PVC/F-MWCNTs membranes have more porous structure than PVDF/PVC membrane and therefore it is expected that their mechanical stability becomes less than that of PVDF/PVC membrane. Similar behavior was reported by Ma et al. [39], who showed that by the incorporation of 0.5–2 wt.% acidic MWCNTs into PVDF membrane, tensile strength decreased due to formation of finger-like pores in sub-layer. Beside, this reduction may be due to stiffness of polymer chains [40]. Interestingly, by augmenting of F-MWCNTs dosage from 0.3 to 1 wt.%, tensile strength increases. This trend implies that F-MWCNTs are properly dispersed in polymer matrix and also they have appropriate interaction with PVDF and PVC chains [41].

3.3. Pure water flux

Fig. 8 illustrates the PWF of blend membranes with different amounts of F-MWCNTs. As can be seen, the PWF is $27.83 \text{ L m}^{-2} \text{ h}^{-1}$ for PVDF50 membrane. When F-MWCNTs dosage augments from 0 to 0.5%, the PWF increases considerably. Nevertheless, further increasing of the filler dosage results in reduction of PWF. For PVDF50-0.3 and PVDF50-0.5, the improve-

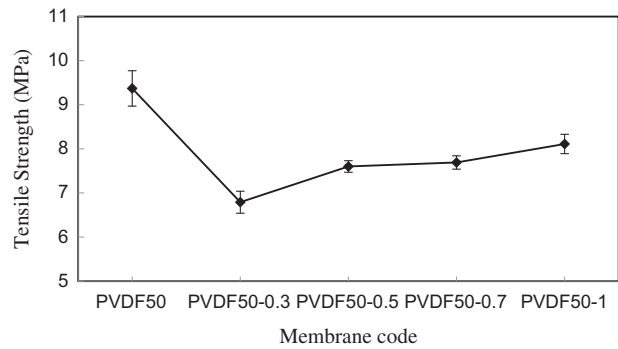


Fig. 7. Tensile strength of prepared membranes.

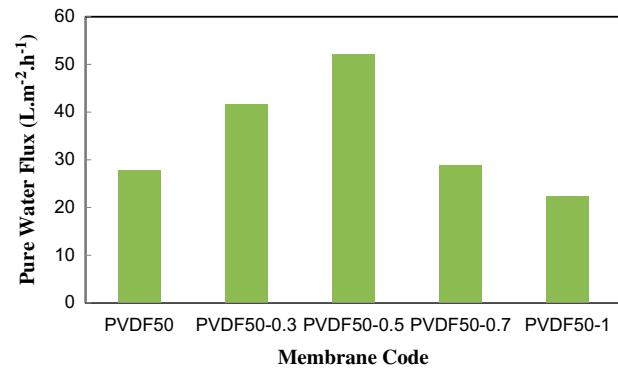


Fig. 8. Effect of F-MWCNTs content on water permeation flux.

ment of PWF can be explained by two factors including hydrophilicity and the pore size of the membrane [42]. The water contact angle results, presented in Table 2, confirm the hydrophilicity enhancement of above-mentioned samples. In this case, the hydrophilic group of F-MWCNTs tempts water molecules to pass through the membrane and as a consequence enhances water flux [43,44]. Moreover, as can be

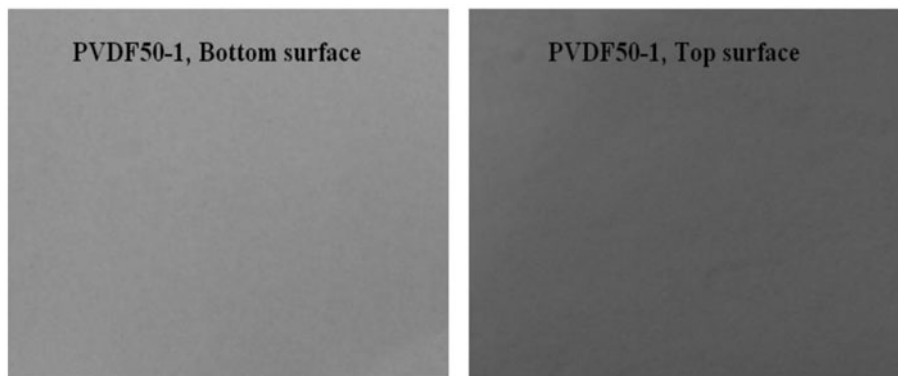


Fig. 6. Digital photographs of top and bottom surface PVDF50-1.

observed in SEM images (Fig. 4), by increasing F-MWCNTs dosage from 0.5 to 1 wt.%, smaller pore sizes are formed which is the dominant factor and decreases PWF. Accordingly, the maximum PWF is achieved for PVDF50–0.5 membrane.

3.4. Permeate flux and dextran rejection

The effect of F-MWCNTs on the performance of PVDF/PVC membrane was studied using dextran removal process. The results of permeate flux are shown in Fig. 9. As illustrated in this figure, permeate flux has changed similarly as PWF for all prepared membranes. Indeed, permeate flux increases up to 0.5 wt.% of F-MWCNTs and then reduces by further increase of F-MWCNTs concentration in casting solution. However, it is noteworthy that permeate flux of each sample decreases comparing to its PWF as a result of fouling effect.

Fig. 10 presents the dextran rejection of the PVDF/PVC and PVDF/PVC/F-MWCNTs membranes. The results show that dextran rejection increases from 41% for PVDF50 to 63.3% for PVDF50–0.3. The enhancement of dextran rejection can be explained by the fact that by addition of 0.3 wt.% F-MWCNTs in casting solution, hydrophilicity increases and water molecules transport faster than dextran through the membrane. However, for PVDF50–0.5, membrane pore size increases and the high water flux drag dextran molecules in permeate [45]. As a result, dextran concentration in permeate side increases and its rejection decreases. However, further increase of F-MWCNTs dosage (0.7–1 wt.%) leads to the more dense structure. In addition, hydrophilicity of PVDF50–0.7 and PVDF50–1 dominates adsorption of dextran molecules on membrane surface and plays a key role in improvement of dextran rejection.

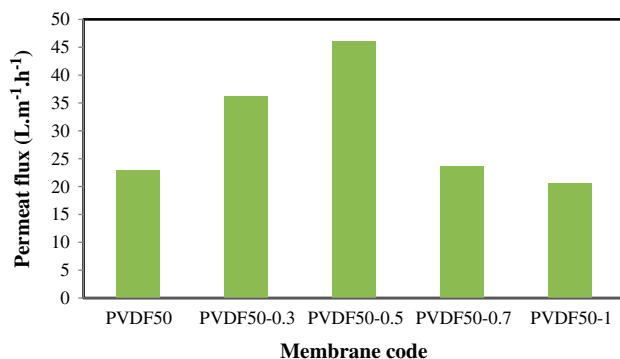


Fig. 9. Effect of F-MWCNTs content on dextran solution flux.

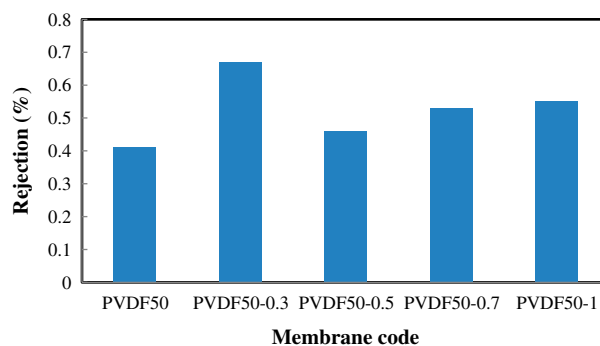


Fig. 10. Rejection of prepared membrane with different loading of F-MWCNTs.

3.5. Antifouling properties of the membranes

The adsorption and deposition of solute on the membrane surface and/or inside pores leads to the formation of membrane fouling which is consisted of reversible and irreversible fouling. Reversible adsorption of solute causes reversible fouling which can be removed by hydraulic cleaning. While, firm adsorption of molecules is the reason of irreversible fouling. The antifouling performance of prepared membranes was characterized by means of measuring water FR after fouling by dextran solution and results are shown in Table 3. As can be observed, FR value for PVDF/PVC/F-MWCNTs membranes increases when compared with PVDF50 membrane. This phenomenon was attributed to increasing surface coverage of the hydrophilic groups on the membrane surface, which could induce denser and more stable hydration layer. From the results, PVDF50–1 membrane possesses the highest FR value of 95 wt.%. According to Table 2, PVDF50–1 membrane has the lowest contact angle and highest hydrophilicity. As a result, its tendency to absorb water molecules increases and adsorption of dextran molecules on the surface becomes less. Besides, the PVDF50–0.7 shows the lowest FR value. In fact, by reducing the pore size of membranes, adsorption of dextran molecules on the surface of pores blocks more pores. This kind of fouling may

Table 3
Antifouling parameters of prepared membranes

Membrane code	FRR (%)	R_{ir} (%)	R_r (%)
PVDF50	82.49	17.50	3.09
PVDF50–0.3	86.105	13.89	–0.47
PVDF50–0.5	87.62	12.37	4.47
PVDF50–0.7	84.3	15.06	3.11
PVDF50–1	95.17	4.82	3.44

hardly eliminates during cleaning process. Interestingly, for PVDF50–0.3, R_r of -0.47 depicted that J_{w2} is lower than permeate flux. This may occur due to blocking of membrane pores by dextran molecules. Accordingly, water flux reduced to the lower level than permeate flux [46].

4. Conclusion

In this work, PVC and F-MWNTs were both introduced to prepare PVDF/PVC/F-MWNTs flat sheet membrane. The effect of F-MWCNTs on the performance of PVDF/PVC membranes was investigated. The F-MWNT exhibited stable dispersion in DMF through sonication. Cross-sectional SEM images of membranes showed that by augmenting F-MWCNTs dosage to 0.5 wt.%, size and number of pores increase, while further increasing of MWCNTs amount led to a denser structure. Embedding F-MWCNTs to PVDF/PVC matrix caused to increase surface hydrophilicity of resultant membrane. Mechanical properties of the prepared membranes were decreased by increasing the F-MWCNTs concentration and then increased. PWF significantly increased by increasing F-MWCNTs loading from 0 to 0.5 wt.%. Beside, PVDF50–0.3 showed the highest rejection dextran value among PVDF/PVC/F-MWCNTs membranes. The results also showed that F-MWCNTs had a positive effect on the antifouling properties of the as-prepared mix matrix membranes.

References

- [1] F. Liu, N.A. Hashim, Y. Liu, M.R.M. Abed, K. Li, Progress in the production and modification of PVDF membranes, *J. Membr. Sci.* 375 (2011) 1–27.
- [2] N. Li, C. Xiao, S. An, X. Hu, Preparation and properties of PVDF/PVA hollow fiber membranes, *Desalination* 250 (2010) 530–537.
- [3] H.P. Srivastava, G. Arthanareeswaran, N. Anantharaman, V.M. Starov, Performance of modified poly(vinylidene fluoride) membrane for textile wastewater ultrafiltration, *Desalination* 282 (2011) 87–94.
- [4] M.H. Razzaghi, A. Safekordi, M. Tavakolmoghadam, F. Rekabdar, M. Hemmati, Morphological and separation performance study of PVDF/CA blend membranes, *J. Membr. Sci.* 470 (2014) 547–557.
- [5] X. Zhao, H. Xuan, C. He, Enhanced separation and antifouling properties of PVDF ultrafiltration membranes with surface covalent self-assembly of polyethylene glycol, *RSC Adv.* 5 (2015) 81115–81122.
- [6] Z.X. Wang, C.H. Lau, N.Q. Zhang, Y.P. Bai, L. Shao, Mussel-inspired tailoring of membrane wettability for harsh water treatment, *J. Mater. Chem. A* 3 (2015) 2650–2657.
- [7] N.A. Hashim, F. Liu, K. Li, A simplified method for preparation of hydrophilic PVDF membranes from an amphiphilic graft copolymer, *J. Membr. Sci.* 345 (2009) 134–141.
- [8] J.H. Li, M.Z. Li, J. Miao, J.B. Wang, X.S. Shao, Q.Q. Zhang, Improved surface property of PVDF membrane with amphiphilic zwitterionic copolymer as membrane additive, *Appl. Surf. Sci.* 258 (2012) 6398–6405.
- [9] C. Zhao, X. Xu, J. Chen, F. Yang, Effect of graphene oxide concentration on the morphologies and antifouling properties of PVDF ultrafiltration membranes, *J. Environ. Chem. Eng.* 1 (2013) 349–354.
- [10] Y. Wei, H.Q. Chu, B.Z. Dong, X. Li, S.J. Xia, Z.M. Qiang, Effect of TiO₂ nanowire addition on PVDF ultrafiltration membrane performance, *Desalination* 272 (2011) 90–97.
- [11] A. Bottino, G. Capannelli, A. Comite, Preparation and characterization of novel porous PVDF-ZrO₂ composite membranes, *Desalination* 146 (2002) 35–40.
- [12] L. Shao, Z.X. Wang, Y.L. Zhang, Z.X. Jiang, Y.Y. Liu, A facile strategy to enhance PVDF ultrafiltration membrane performance via self-polymerized polydopamine followed by hydrolysis of ammonium fluorotitanate, *J. Membr. Sci.* 461 (2014) 10–21.
- [13] J. Xu, Z.L. Xu, Poly(vinyl chloride) (PVC) hollow fiber ultrafiltration membranes prepared from PVC/additives/solvent, *J. Membr. Sci.* 208 (2002) 203–212.
- [14] X. Zhang, Y. Chen, A.H. Konsowa, X. Zhu, J.C. Crittenden, Evaluation of an innovative polyvinyl chloride (PVC) ultrafiltration membrane for wastewater treatment, *Sep. Purif. Technol.* 70 (2009) 71–78.
- [15] Q. Zhang, S. Zhang, Y. Zhang, X. Hu, Y. Chen, Preparation of PVDF/PVC composite membrane for wastewater purification, *Desalin. Water Treat.* 51 (2013) 3854–3857.
- [16] R. Wang, K. Hashimoto, A. Fujishima, M. Chikuni, E. Kojima, A. Kitamura, M. Shimohigoshi, T. Watanabe, Photogeneration of highly amphiphilic TiO₂ surfaces, *Adv. Mater.* 10 (1998) 135–138.
- [17] Z. Rajabi, A.R. Moghadassi, S.M. Hosseini, M. Mohammadi, Preparation and characterization of polyvinylchloride based mixed matrix membrane filled with multi walled carbon nano tubes for carbon dioxide separation, *J. Ind. Eng. Chem.* 19 (2013) 347–352.
- [18] J. Wang, W.Z. Lang, H.P. Xu, X. Zhang, Y.J. Guo, Improved poly(vinyl butyral) hollow fiber membranes by embedding multi-walled carbon nanotube for the ultrafiltrations of bovine serum albumin and humic acid, *Chem. Eng. J.* 260 (2015) 90–98.
- [19] P. Daraei, S.S. Madaeni, N. Ghaemi, H.A. Monfared, M.A. Khadivi, Fabrication of PES nanofiltration membrane by simultaneous use of multi-walled carbon nanotube and surface graft polymerization method: Comparison of MWCNT and PAA modified MWCNT, *Sep. Purif. Technol.* 104 (2013) 32–44.
- [20] C.P. Bergmann, M. Jung de Andrade, *Nanostructured Materials for Engineering Applications*, Springer, Berlin, 2011.
- [21] J. Leng, A.K.T. Lau, *Multifunctional Polymer Nanocomposites*, CRC Press, New York, NY, 2011.
- [22] L. Qu, Y. Lin, D.E. Hill, B. Zhou, W. Wang, X. Sun, A. Kitaygorodskiy, M. Suarez, J.W. Connell, L.F. Allard, Y.P. Sun, Polyimide-functionalized carbon nanotubes:

- Synthesis and dispersion in nanocomposite films, *Macromolecules* 37 (2004) 6055–6060.
- [23] A. Eitan, K. Jiang, D. Dukes, R. Andrews, L.S. Schadler, Surface modification of multiwalled carbon nanotubes: Toward the tailoring of the interface in polymer composites, *Chem. Mater.* 15 (2003) 3198–3201.
- [24] K. Balasubramanian, M. Burghard, Chemically functionalized carbon nanotubes, *Small* 1 (2005) 180–192.
- [25] X. Zhao, J. Ma, Z. Wang, G. Wen, J. Jiang, F. Shi, L. Sheng, Hyperbranched-polymer functionalized multi-walled carbon nanotubes for poly (vinylidene fluoride) membranes: From dispersion to blended fouling-control membrane, *Desalination* 303 (2012) 29–38.
- [26] X. Zhang, W.Z. Lang, H.P. Xu, X. Yan, Y.J. Guo, L.F. Chu, Improved performances of PVDF/PFSA/O-MWNTs hollow fiber membranes and the synergism effects of two additives, *J. Membr. Sci.* 469 (2014) 458–470.
- [27] K.A. Wepasnick, B.A. Smith, K.E. Schrote, H.K. Wilson, S.R. Diegelmann, D.H. Fairbrother, Surface and structural characterization of multi-walled carbon nanotubes following different oxidative treatments, *Carbon* 49 (2011) 24–36.
- [28] H. Susanto, M. Ulbricht, Influence of ultrafiltration membrane characteristics on adsorptive fouling with dextrans, *J. Membr. Sci.* 266 (2005) 132–142.
- [29] G.D. Vuković, A.D. Marinković, M. Čolić, M.Đ. Ristić, R. Aleksić, A.A. Perić-Grujić, P.S. Uskoković, Removal of cadmium from aqueous solutions by oxidized and ethylenediamine-functionalized multi-walled carbon nanotubes, *Chem. Eng. J.* 157 (2010) 238–248.
- [30] R. Yu, L. Chen, Q. Liu, J. Lin, K.L. Tan, S.C. Ng, H.S.O. Chan, G.Q. Xu, T.S.A. Hor, Platinum deposition on carbon nanotubes via chemical modification, *Chem. Mater.* 10 (1998) 718–722.
- [31] S. Rajendran, P. Sivakumar, R.S. Babu, Studies on the salt concentration of a PVdF-PVC based polymer blend electrolyte, *J. Power Sources* 164 (2007) 815–821.
- [32] S. Rajendran, P. Sivakumar, An investigation of PVdF/PVC-based blend electrolytes with EC/PC as plasticizers in lithium battery applications, *Physica B* 403 (2008) 509–516.
- [33] S.S. Madaeni, S. Zinadini, V. Vatanpour, Convective flow adsorption of nickel ions in PVDF membrane embedded with multi-walled carbon nanotubes and PAA coating, *Sep. Purif. Technol.* 80 (2011) 155–162.
- [34] V. Vatanpour, S.S. Madaeni, R. Moradian, S. Zinadini, B. Astinchap, Novel antifouling nanofiltration polyethersulfone membrane fabricated from embedding TiO₂ coated multiwalled carbon nanotubes, *Sep. Purif. Technol.* 90 (2012) 69–82.
- [35] H. Wu, B. Tang, P. Wu, Novel ultrafiltration membranes prepared from a multi-walled carbon nanotubes/polymer composite, *J. Membr. Sci.* 362 (2010) 374–383.
- [36] V. Vatanpour, M. Esmaeili, M.H.D. Abdi, Fouling reduction and retention increment of polyethersulfone nanofiltration membranes embedded by amine-functionalized multi-walled carbon nanotubes, *J. Membr. Sci.* 466 (2014) 70–81.
- [37] N. Pezeshk, D. Rana, R.M. Narbaitz, T. Matsuura, Novel modified PVDF ultrafiltration flat-sheet membranes, *J. Membr. Sci.* 389 (2012) 280–286.
- [38] E. Celik, H. Park, H. Choi, H. Choi, Carbon nanotube blended polyethersulfone membranes for fouling control in water treatment, *Water Res.* 45 (2011) 274–282.
- [39] J. Ma, Y. Zhao, Z. Xu, C. Min, B. Zhou, Y. Li, B. Li, J. Niu, Role of oxygen-containing groups on MWCNTs in enhanced separation and permeability performance for PVDF hybrid ultrafiltration membranes, *Desalination* 320 (2013) 1–9.
- [40] V.J. Mkhabela, A.K. Mishra, X.Y. Mbianda, Thermal and mechanical properties of phosphorylated multi-walled carbon nanotube/polyvinyl chloride composites, *Carbon* 49 (2011) 610–617.
- [41] C.M. Chang, Y.L. Liu, Functionalization of multi-walled carbon nanotubes with non-reactive polymers through an ozone-mediated process for the preparation of a wide range of high performance polymer/carbon nanotube composites, *Carbon* 48 (2010) 1289–1297.
- [42] V. Vatanpour, S.S. Madaeni, R. Moradian, S. Zinadini, B. Astinchap, Fabrication and characterization of novel antifouling nanofiltration membrane prepared from oxidized multiwalled carbon nanotube/polyethersulfone nanocomposite, *J. Membr. Sci.* 375 (2011) 284–294.
- [43] H.P. Ngang, B.S. Ooi, A.L. Ahmad, S.O. Lai, Preparation of PVDF-TiO₂ mixed-matrix membrane and its evaluation on dye adsorption and UV-cleaning properties, *Chem. Eng. J.* 197 (2012) 359–367.
- [44] J.H. Choi, J. Jegal, W.N. Kim, Fabrication and characterization of multi-walled carbon nanotubes/polymer blend membranes, *J. Membr. Sci.* 284 (2006) 406–415.
- [45] S. Majeed, D. Fierro, K. Buhr, J. Wind, B. Du, A. Boschetti-de-Fierro, V. Abetz, Multi-walled carbon nanotubes (MWCNTs) mixed polyacrylonitrile (PAN) ultrafiltration membranes, *J. Membr. Sci.* 403 (2012) 101–109.
- [46] J.P.F. De Bruijn, F. N. Salazar, R. Bo´rquez, Membrane blocking in Ultrafiltration, *Food Bioprod. Process.* 83 (2005) 211–219.